

THE DAMPING OF WATER WAVES BY INSOLUBLE ORGANIC MONOLAYERS

W. D. Garrett
Surface Chemistry Branch
Chemistry Division

and

J. D. Bultman
Organic and Biological Chemistry Branch
Chemistry Division

October 17, 1963

APPROVED FOR PUBLIC
RELEASE - DISTRIBUTION
UNLIMITED



U. S. NAVAL RESEARCH LABORATORY
Washington, D.C.

CONTENTS

Abstract	ii
Problem Status	ii
Authorization	ii
HISTORICAL BACKGROUND	1
THEORETICAL CONSIDERATION	2
APPARATUS	4
EXPERIMENTAL PROCEDURE	5
Circular Waves	6
Plane Waves	6
DAMPING OF WATER WAVES BY INSOLUBLE MONOLAYERS	7
DISCUSSION AND CONCLUSIONS	14
REFERENCES	17

ABSTRACT

The damping of capillary waves (wavelength < 1.0 cm) by insoluble organic monolayers has been examined in detail at low film pressure. The experimental system was designed to (a) generate either circular or plane waves at various frequencies and amplitudes, (b) measure the wave amplitudes, and (c) provide for the addition and removal of insoluble monolayers and the measurement and control of monolayer film pressure. Force vs area curves were also determined for all pure compounds studied and these data were compared with the wave-damping results.

The damping coefficient k was found to increase slowly as the monolayer was compressed at film pressures < 0.1 dyne/cm. Between approximately 0.1 and 0.5 dyne/cm there was an abrupt rise in k to a maximum value which remained essentially constant with increasing film pressure. After the film pressure had reached about 0.5 dyne/cm, little additional damping occurred when more material was added to the surface. A comparison of wave-damping data with force vs area curves indicated that the sudden increase in the damping coefficient occurred in the neighborhood of the region of transition of the monolayer from a gaseous film to a more condensed state. A similar relationship was found between the damping coefficient and the modulus of surface compressibility where the rapid rise of k occurs at compressibility modulus values of from 0.02 to 0.13 dyne/cm. All compounds studied behaved similarly with respect to these wave-damping relationships even though they differed markedly in chemical structure.

PROBLEM STATUS

This is an interim report; work is continuing on the problem.

AUTHORIZATION

NRL Problem C02-18
BUWEP Task No. RUDC-4B-000/652-1/S031-01-00-231-3

Manuscript submitted July 29, 1963.

THE DAMPING OF WATER WAVES BY INSOLUBLE ORGANIC MONOLAYERS

HISTORICAL BACKGROUND

For centuries mariners have observed areas of the oceans in which the small wave structure has been damped. It has long been known that these surface scars, known as sea slicks, could be artificially produced by pouring various oils onto the surface of the water. Fish oils and oxidized petroleum oils have been commonly used to calm wind-generated small amplitude waves, improve the transmission of light through the water surface, and reduce the breaking of waves and surf. Interesting accounts of the history of sea slicks and wave-calming oils are found in papers by Davies (1) and Banting (2).

Early scientific interest in these phenomena goes back to 1862, when Thomson (3) discussed the origin of "calm lines often seen on a rippled sea." In 1891 Pockels (4) demonstrated experimentally for the first time that small (capillary) waves could be damped by various surface active materials. An attempt to find a mechanism for wave damping was made in the late nineteenth century by Aitken (5), who performed several experiments designed to measure the physical effects of oil films on water surfaces. Reynolds (6) theorized that an elastic surface film dissipated wave energy due to the alternating tangential drag on the water as the surface is expanded and contracted by the passing crests and troughs. This concept was expressed mathematically by Lamb (7). Shuleikin (8) described several carefully conducted experiments concerning the damping of capillary waves. He concluded (a) that damping is not due to a reduced surface tension and (b) it is not caused by a decrease in the coefficient of friction between the air and the water due to the presence of a surface film. It was furthermore concluded that the damping caused by fatty acids should be greater on sea water than on fresh water because of soap formation, which would produce a more rigid film.

A number of marine investigators (9-12) have measured the film pressure "in situ" of many naturally occurring sea slicks using the spreading-oil method of Adam (13). Film pressures in many slicks were quite low (2 to 10 dynes/cm), giving rise to the concept that damping of wind-generated waves can occur with only partially compressed monolayers of surface active materials. Ewing (14) has discussed the action of internal waves by which surface compressional forces are formed which are sufficient to create slicks by packing the amphipathic molecules existing at the sea surface. The resulting partially compacted film decreased the magnitude of the small waves, giving rise to a visibly modified area of the sea surface.

In recent years, a number of studies of the wave-damping mechanism have been reported. Goodrich (15,16) examined several condensed monolayers and found less attenuation than would be anticipated from Lamb's hypothesis. A somewhat similar study was conducted by Vines (17) who found wave damping by condensed surface films in excess of that predicted by Lamb's theory for a film covered surface. A survey paper by Davies (1) reviews wave-damping data and theory for surfaces covered by both insoluble monolayers and soluble surface active materials capable of adsorbing at the air/water interface. In the latter category, several papers have reported that a damping maximum exists as the concentration of soluble surfactant is increased (18-21). At concentrations above that maximum the wave attenuation rate decreases. Dorrestein (22) has analyzed these effects mathematically and derived expressions relating wave damping to surface viscosity and the surface compressional modulus.

The existing literature contains several theoretical approaches to this problem. Much of the experimental data upon which these mathematical analyses are based is for condensed films or upon systems involving soluble surface active agents for which film pressures are unspecified. The effect of varying film pressure on wave damping has not been sufficiently explored, especially in the very low pressure range. Surface viscosity and surface compressional modulus data are also needed for films whose damping characteristics have been measured in order to substantiate or disprove the existing mechanisms.

THEORETICAL CONSIDERATION

According to Lord Kelvin (23), the velocity v of a surface wave on a liquid in a large and deep basin is given by

$$v^2 = \frac{g\lambda}{2\pi} + \frac{2\pi\gamma}{\rho\lambda} \quad (1)$$

where λ is the wavelength, g is the gravitational constant, γ is the surface tension, and ρ the density of the liquid. For values of λ less than 1.0 cm, the first term of Eq. (1), the gravitational term, is small in comparison with the second term, the capillary term. Hence, as surface tension is reduced, the velocity of capillary waves decreases. From the Kelvin expression it can be shown that on a clean water surface the amplitudes of plane waves originating from an infinitely long linear source follow an exponential decay expression

$$a = a_0 e^{-kx} \quad (2)$$

where a_0 is the amplitude of the wave at the source and x is the distance from the source. The damping coefficient is k , which according to theory can be calculated from

$$k = \frac{8\pi^2\eta}{\rho v\lambda^2} \quad (3a)$$

or, as an approximation

$$k = \frac{8\pi\eta f}{3\gamma} \quad (3b)$$

where v is the group velocity of the wave-train, f is the ripple frequency, and η is the bulk viscosity expressed in poises. The second expression is valid only for water and short wavelengths (0.5 cm or less).

In circular waves originating from a point source, energy loss is associated with the expansion of the circular wave front in addition to the restoring forces embodied in k in Eq. (2). For this reason, it is to be expected that circular wave amplitudes decrease faster than plane wave amplitudes until the circular waves reach a distance from the source where they can be treated as essentially planar.

The previously discussed relationships for the damping of plane waves hold only for clean water surfaces. As surface active materials are spread upon or adsorb at the surface,

modifications of the various surface properties occur. The resulting immobilization of the liquid surface has been considered by several workers to be the major contributing factor explaining the greater damping coefficient observed for a film-covered surface. The damping coefficient k for a surface immobilized by a close packed monolayer may be expressed according to Davies (1) as

$$k = \left(\frac{\pi}{v\lambda} \right) \left(\frac{\eta\sigma}{2\rho} \right)^{1/2} \quad (4)$$

where

$$\sigma = \left(\frac{2\pi g}{\lambda} + \frac{8\pi^3 \gamma}{\lambda^3 \rho} \right)^{1/2}.$$

By comparison of Eq. (4) with Eq. (3a) it can be shown that the damping coefficient is increased by $(\lambda/8\pi\sqrt{2}) (\rho\sigma/\eta)^{1/2}$ for the immobilized surface over that for the clean surface. This ratio becomes approximately 2 for wavelengths in the neighborhood of 0.5 cm. Obviously a highly dilute insoluble monolayer does not produce a wholly immobilized surface, yet fragmentary evidence in the literature has indicated that damping does occur at extremely low film pressures. Thus it would appear that Eq. (4) which contains no surface parameters other than surface tension, is not applicable to low pressure films.

Various surface parameters such as the surface viscosity and the modulus of surface compressibility $-AdF/dA$ dyne/cm have been utilized in mathematical analyses to describe wave damping over broader ranges of surface conditions. Davies (24) derived a damping expression which includes a term for the dissipation of wave energy by viscous bulk forces plus a term which considers surface compressional effects. Dorrestein (22) obtained an expression which accounts for surface viscosity as well as the surface compressional modulus in describing capillary wave damping. Davies (1) has pointed out that these theoretical analyses agree to a reasonable extent with the limited experimental evidence available.

In explaining capillary-wave-damping phenomena it is necessary to account for the energy dissipated when a monolayer smooths an otherwise rippled water surface. One energy sink available is the result of coupling between the molecules of the monolayer and those of the substrate, resulting in a viscous drag or lack of slippage as the monolayer and the substrate move with respect to each other. The existence of such an effect was first demonstrated by Schulman and Teorell (25) when they found that a layer of water approximately 0.03 mm deep was transported when an oleic acid monolayer moved across the water surface. Their result indicates an appreciable monolayer-water association involving no doubt the hydrogen bonding of a large number of water molecules with the hydrophilic polar groups of the monolayer. This entire associated system would have to be moved and would offer resistance to the expansions and contractions of the liquid surface with the passage of waves.

In order to substantiate the preceding mechanism, the effect of insoluble monolayers on wave damping at very low film pressures must be established and the transition from the clean surface to the immobilized situation studied. It was the purpose of this investigation to find the effect of adsorbed insoluble monolayers on wave damping as a function of film pressure or other pertinent surface parameters for various interesting classes of pure surface active compounds.

APPARATUS

An experimental system was constructed which (a) generates circular or plane waves, (b) measures their amplitudes, (c) provides means for the addition and removal of insoluble monolayers from the water surface, and (d) allows the film pressure to be measured and controlled. The assembly, schematized in Fig. 1, is patterned after a device described in an NRL Report by Schooley (26). A signal generated by an audio oscillator was amplified and fed into an electromechanical transducer which vibrates either a pin head or a linear knife edge in the surface of water contained in a glass ripple tank. The pin head was coated lightly with paraffin wax to reduce wave distortions caused by adhesion of the water to the pin metal. Plane waves were generated by a rigid 45-degree knife edge (20 cm long) made from polymethyl methacrylate. The signal from the oscillator passed through an impedance matching device and an attenuator which provided a means of varying the wave amplitudes. The same signal source of emf applied to the wave generator was also used without attenuation to drive a synchronous motor which turned a light-chopper disk. The disk slots and motor speed were chosen so that the number of chops per second was identical to the applied frequency. Light from a 150-watt projection lamp passing through the chopper was therefore interrupted at the same frequency as that of the water waves generated in the trough. Hence, with this stroboscopic arrangement, the observer saw a system of standing waves. The light rays upon passing upward through the rippled surface were converged by the wave crests and an optical standing wave pattern was projected onto a translucent plastic screen above the glass ripple tank.

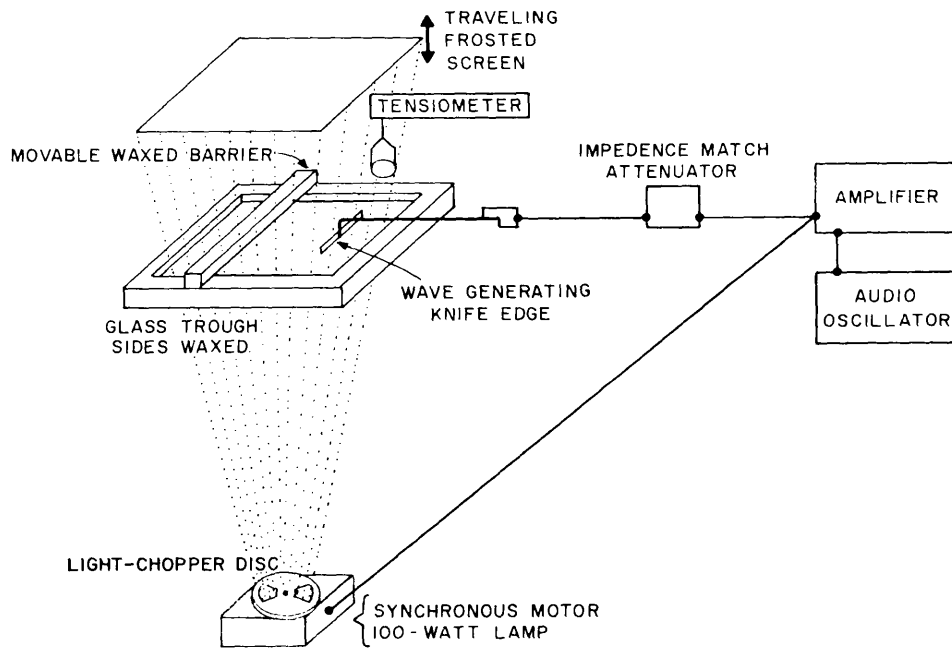


Fig. 1 - Schematic of the wave generation and amplitude measuring system

The 1-cm-deep glass trough was also arranged to serve as a film balance. The sides of the 50 by 50 cm square trough were coated with clean, white, high-melting paraffin wax, which allowed the tank to be overfilled to some extent without spillage. Waxed sliding barriers were used to sweep the water surface to compress existing monolayers or to

remove unwanted surface film, such as oily contaminants. Another valuable feature of this arrangement was that the downward curving water surface at the water-paraffin boundary appeared to act as a reverse beach, thereby reducing wave reflections from the sides of the tank. A Cenco du Nouy surface tensiometer was used to measure the surface tension of the water. As is well known, the difference between the surface tension of a film-covered surface and that of a clean water surface is equal to the pressure of the surface film. The trough depth of one centimeter was chosen to conserve distilled water and to reduce the time required for soluble impurities to reach the surface where they were removed by the surface sweeping technique described above. Lord Rayleigh (27) discussed corrections which had to be applied to wave properties of water contained in shallow containers; however, for the 0.52-cm wavelengths generally used in this work, the depth correction is not significant.

The calculation of wave amplitude is derived from the light path diagram depicted in Fig. 2. Light passing through a wave crest is refracted and focused at a point above the water surface. The greater the wave amplitude, the shorter is the focal length of the transmitted ray. When the plastic screen is placed near the water surface below the focal point, a diffuse pattern is seen. At the focal point a sharp bright pattern results, and as the screen is raised above the focal point the image widens but remains rather sharp. Schooley (26) derived from the optical geometry the following approximate expression for the wave amplitude

$$a = 0.15\lambda^2 \left(\frac{1}{L_1} + \frac{1}{L_2} + \frac{3w}{\lambda L_3} \right). \quad (5)$$

The amplitude a is expressed in terms of L_1 , L_2 , and L_3 which are the distances from the water surface to the light source, the screen, and the focal point, respectively. Here w is the width of the bright image. The above expression holds when the screen is above the focal point. In this investigation the screen was placed at the focal point for each wave measured. In this instance $w = 0$ and the amplitude equation becomes

$$a = 0.15\lambda^2 \left(\frac{1}{L_1} + \frac{1}{L_2} \right). \quad (6)$$

Since L_1 is fixed, the amplitudes are an inverse function of the height of the screen at which a wave pattern just becomes sharp and bright. Wavelengths were measured by placing the screen at the water surface and measuring the spacing between the waves nearest the wave generator. The wavelength decrease with distance is small for the wavelengths studied. Consequently, there is little error induced into the amplitude measurement by determining wavelength in this fashion.

EXPERIMENTAL PROCEDURE

The glass trough was thoroughly cleaned and filled with water so that the water level was above that of the waxed edge. A waiting period of one hour was normally used so that soluble surface active impurities could diffuse to and adsorb at the surface. During this time the trough was kept covered to eliminate contamination of the surface by airborne materials. The surface was then swept several times with a barrier coated with paraffin wax to assure cleanliness. Fine floating particles of Teflon powder were sprinkled on the surface and observed as the barrier crossed the trough. Only when the particles collected in front of the barrier was the water surface presumed clean. If any surface impurity existed, the Teflon particles remained with the surface film and traveled ahead of the

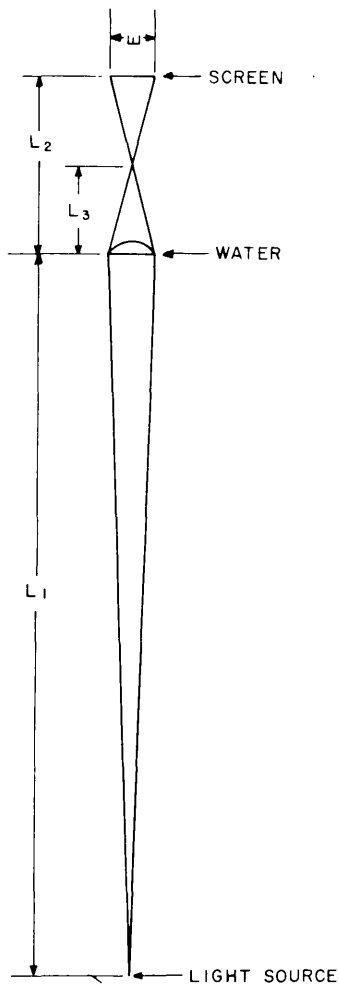


Fig. 2 - Geometry of ripple focusing

barrier. The surface tension of the clean water was measured by the du Noüy ring method using a 6.0-cm-diameter platinum ring. Circular or plane waves were generated at a selected frequency and amplitude with the generating probe just touching the water surface. Unsatisfactory wave patterns were formed when the probe tip was submerged. Since experimental procedures depended upon the type of waves generated, they will be considered separately. All experiments were performed in a 25°C constant temperature room.

Circular Waves

The waxed pin head oscillating perpendicularly to the surface at 60 cycles/sec generated a series of concentric circular waves whose amplitudes were determined by the method described in the previous section (Eq. 6). The successive wave amplitudes were measured from the probe along a radial straight line for a distance of at least 5 cm. Circular wave data are presented by plotting the logarithm of the amplitude versus radial distance from the wave source. When the water surface was clean, a straight line plot resulted. As minute quantities of surface active impurities found their way into the surface, additional damping occurred and the semilog plots deviated from rectilinearity. Both this property and the absolute value of the surface tension were used as criteria of surface purity. It was found that water in a clean trough could be maintained in a clean condition for several hours, which was sufficient time to complete an experiment.

Fractions of a condensed monolayer were carefully formed by spreading onto the clean water surface small measured volumes of a dilute solution of a surface active compound in chloroform or petroleum ether. Since most of this work was primarily concerned with low film pressures, irreproducibility of monolayer properties due to the incorporation in the film of unevaporated solvent such as reported

by Archer and Lamer (28) in stearic acid films was not encountered. Wave amplitudes, wavelength, and surface tension, from which film pressures are calculated, were determined after each addition of the surface active agent to the monolayer on the water surface.

Plane Waves

Using the polymethyl methacrylate straight edge for wave generation, plane waves were generated at a frequency of 60 cycles/sec with a wavelength of 0.52 cm. The measurements and calculations of the individual wave amplitudes were performed in a manner identical to that for the circular waves. However, since there were no complicating effects of an expanding wave front as with circular waves, the plane wave measurements could be made at any point along the wave train. Linear plots of $\log a$ versus distance were obtained for both clean and film-covered surfaces. It was not possible, therefore, to use the linearity of the plot as a criterion of cleanliness. Instead, the damping coefficient was calculated from the slope of the linear plot and compared with the theoretical value calculated from Eq. (3). Only when the surface was completely free of surface active materials would the theoretical and experimental damping coefficients agree closely.

DAMPING OF WATER WAVES BY INSOLUBLE MONOLAYERS

According to the previously discussed theories, capillary wave damping is dependent upon various physical parameters of the bulk substrate and the surface film. Damping attributed to molecular structural peculiarities of surface active agents in the film may be demonstrated by varying the hydrophilic functional groups of the molecules studied. In order to establish this, a series of monolayer forming materials containing different functional groups was studied on synthetic sea water (29) using circular waves. The composition of the synthetic sea water is given in Table 1.

Table 1
Composition of Synthetic Sea Water *

Salt	Grams per Liter
NaCl	24.54
MgCl ₂ ·6H ₂ O	11.10
Na ₂ SO ₄	4.09
CaCl ₂	1.16
KCl	0.69
NaHCO ₃	0.20
KBr	0.10
SrCl ₂ ·6H ₂ O	0.04
H ₃ BO ₃	0.03
NaF	0.003

*The pH of the sea water solution is adjusted to 8.0 with 0.1 N Na₂CO₃.

A typical plot of $\log a$ versus distance from the wave source is shown in Fig. 3 for pure oleyl alcohol spread as a monolayer on sea water. Wave attenuation on a clean sea water surface led to a straight line plot of amplitude versus distance. The calculated damping coefficient was 0.10. From Fig. 3 it can be noted that as the monolayer was added to the surface, the amplitudes fell off sharply along a curved line which became more rectilinear with the radial distance. As the surface active material was added to form the monolayer on the water surface, no apparent additional damping was noticed until the film became sufficiently coherent to manifest a measurable film pressure. After this stage was reached, damping commenced with the largest effects taking place at low film pressures. After the film pressure had reached 1 to 2 dynes/cm, little additional damping occurred when more material was added to the surface.

Since the slopes of the amplitude vs distance plots became more linear with distance, a point was chosen arbitrarily at 5.0 cm from the wave source for a comparison of the extent to which damping had occurred for various film pressures. Amplitude values at 5.0 cm for a damped condition were divided by the clean water amplitude at the same distance to obtain a fractional value, a/a_0 . In Fig. 4, the value of $(1 - a/a_0)$ is plotted against film pressure

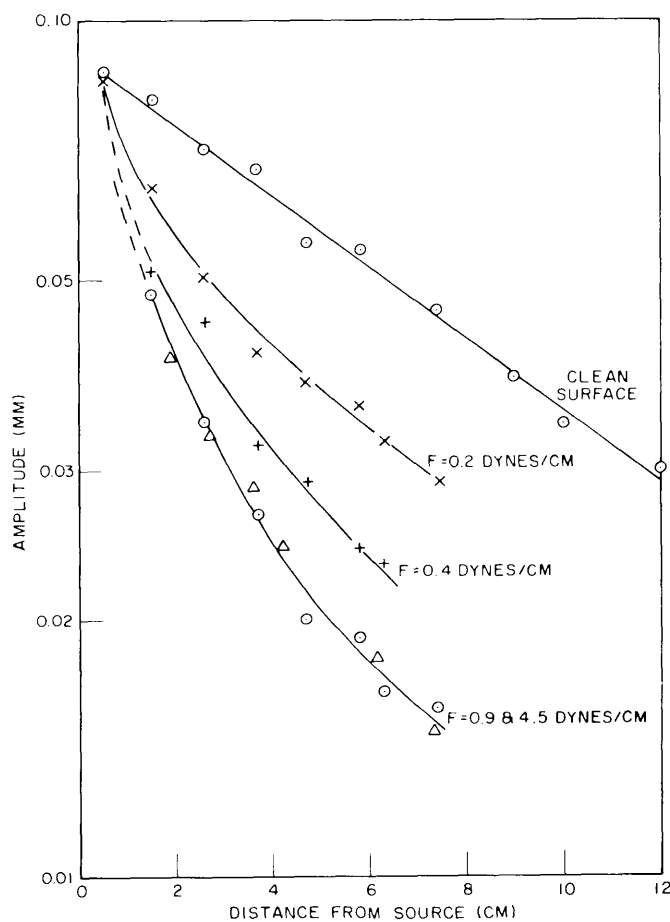


Fig. 3 - Damping of circular waves on synthetic sea water by an oleyl alcohol monolayer at various film pressures

for a number of insoluble surface active compounds on synthetic sea water. Results are plotted over a range of only 4 dynes/cm in order to give sufficient detail in the region of low film pressures. The degree of damping increases rapidly with film pressure and levels out at approximately 1 dyne/cm, becoming essentially constant thereafter. Furthermore, since all types of monolayers studied fall on or near the drawn curve, effects due to differences in molecular structure are either small or absent. Above pressures of 4 dynes/cm the degree of damping remained constant within the accuracy of this technique. All monolayers were measured at film pressures up to 10 to 15 dynes/cm.

Most wave-damping studies in the literature have been performed using plane waves generated by an oscillating linear-wave generator. In addition, as previously discussed, several theoretical analyses of wave damping have been applied to this wave form. For these reasons plane waves were used in the study of damping caused by several pure compounds. Twice-distilled 9, (and 10)-phenylstearic acid (Eastern Regional Research Laboratory) was studied on distilled water, synthetic sea water, and sulfuric acid solution (pH 2). The data for 9, (and 10)-phenylstearic acid are in Table 2. The phenyl derivative was selected to avoid formation of adlineated clusters of molecules at low film pressures. The following materials were studied on synthetic sea water; oleyl alcohol (University of Wisconsin), cetyl alcohol (Eastman No. 1324), triolein (Mann Research Laboratories), oleic

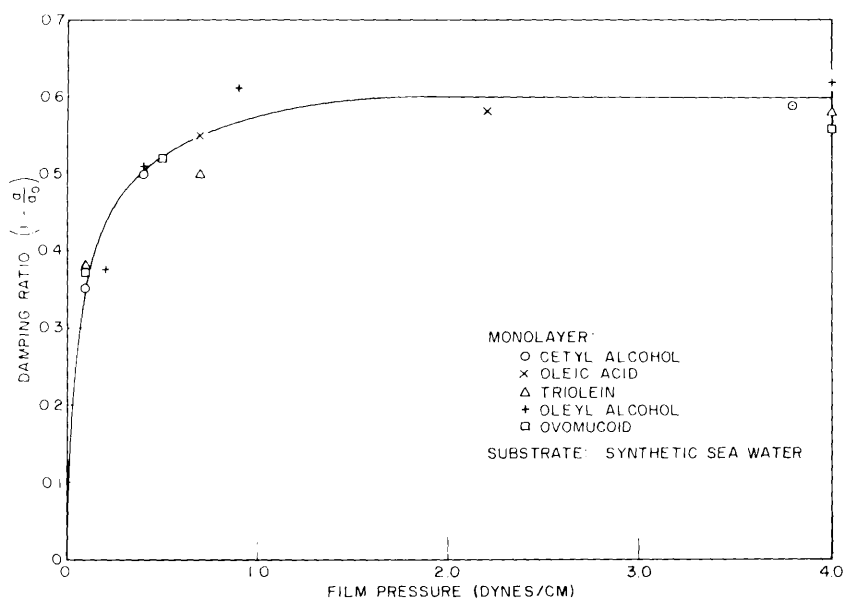


Fig. 4 - The relationship between film pressure and damping of circular waves

acid (Hormel Foundation-prepared from highly purified methyl oleate by saponification and distillation), and crystalline ovomucoid (Mann Research Laboratory, mol wt 28,800 g/mole). The ovomucoid was spread from aqueous buffer solution (pH 7).

Typical plane wave decay data are graphed in Fig. 5 for ovomucoid on synthetic sea water, where the log of the amplitude is plotted against distance along the wave path. The slope of the resulting straight line is related to the damping coefficient through Eq. (2):

$$k = \frac{(\log a_0 - \log a) (2.303)}{x}$$

The damping coefficient for a clean distilled water surface at 25°C was found to be 0.065. This compared favorably with the theoretical value of $k = 0.062$ calculated from Eq. (3). The damping coefficients measured for the clean synthetic sea water (density = 1.024 g/cc, viscosity = 0.0103 poise) are in Table 3. As the monolayer was spread onto the water surface, wave damping began at film pressures lower than could be adequately measured by the ring method (<0.1 dyne/cm). The damping coefficient increased with subsequent additions of ovomucoid. As was found in the experiment with circular waves, the greatest wave-damping effects occurred at very low film pressures, with k rapidly approaching a maximum as the pressure increased.

In order to compare these data with other surface parameters, graphs of film pressure (F) vs area per molecule (A) of the compounds were determined on the appropriate water substrates. These F vs A measurements were made on a modified Wilhelmy film balance in which the film is spread on an aqueous substrate between adjustable barriers. Film pressures were measured as surface tension reductions of the film-covered substrate. The reductions appeared as changes in apparent buoyancy of a platinum slide of known perimeter suspended from the beam of an analytical balance and hanging edgewise in the liquid (30,31). Modifications made included the null-point method of Ruysen (32), the electromagnetic

Table 2
Comparison of Damping Coefficient with Film Pressure and Modulus of Surface Compressibility for 9, (and 10)-Phenylstearic Acid Monolayers on Various Substrates

Sea Water			Acid Water			Distilled Water		
F (dynes/cm)	k (cm ⁻¹)	$\frac{-A\delta F^*}{dA}$	F (dynes/cm)	k (cm ⁻¹)	$\frac{-A\delta F^*}{dA}$	F (dynes/cm)	k (cm ⁻¹)	$\frac{-A\delta F^*}{dA}$
-	0.060	-	-	0.056	-	-	0.055	-
0.1	0.070	0.32	0.1	0.076	0.37	0.2	0.086	0.22
1.2	0.24	5.9	0.15	0.083	0.43	0.4	0.20	0.80
3.9	0.24	22	0.25	0.25	1.1	3.2	0.24	21
			1.0	0.26	7.7	16.0	0.24	-
			3.0	0.26	27			
			4.4	0.26	30			
			8.2	0.27	31			
			16.8	0.30	-			

*Data for modulus of surface compressibility taken from force vs area curve at a molecular area corresponding to that of the wave-damping data.

device of Augenstine (33) for measuring the restoring force, and the Teflon tray and barriers of Fox and Zisman (34). A simple optical lever about 19 feet long served to indicate displacement. The electromagnetic pull necessary to restore balance was measured as an IR drop across a standard resistor. From calibration data, millivolt values were converted to film pressures in dynes/cm. A more detailed description of this apparatus was reported by Bultman (35).

The F vs A curves were determined for each of the six pure compounds. These monolayers were spread from the same dilute solutions used in the wave-damping experiments. As a further precaution, portions of the same water stock solutions were used as the aqueous substrate in both the film balance and wave-damping experiments. Special emphasis was given to the low film pressure region, since damping had been found to occur with the first addition of surface active material and experienced its greatest changes at film pressures of less than 1 dyne/cm. All of these monolayers were "gaseous" at low film pressures on the substrates studied.

The data from the wave-damping apparatus were related with those obtained by the Wilhelmy balance. From the amount of material spread onto the wave trough, molecular areas were calculated for each film pressure at which the wave damping was studied. Film pressure and modulus of surface compressibility values were taken from the F vs A curve at the same molecular area. These data together with the corresponding damping coefficients measured during the wave-damping experiment are compared in Tables 2 and 3. Since the measured film pressure values generally agreed with those determined from the F vs A curve at the same molecular area, it was assumed that it was valid to apply the compressibility values to the wave-damping data.

Table 3
Comparison of Damping Coefficient with Film Pressure and Modulus of Surface Compressibility
for Various Monolayers on Substrate of Synthetic Sea Water

Oleic Acid			Oleyl Alcohol			Ovomucoid			Cetyl Alcohol			Triolein		
F (dynes/cm)	k (cm ⁻¹)	$\frac{-AdF^*}{dA}$												
-	0.060	-	-	0.068	-	-	0.065	-	-	0.062	-	-	0.065	-
< 0.1	0.077	0.17	< 0.1	0.087	0.10	< 0.1	0.081	0.4	< 0.1	0.082	0.14	< 0.1	0.11	0.14
0.1	0.091	0.4	0.15	0.11	0.14	0.1	0.11	0.5	0.1	0.12	0.27	0.15	0.18	0.73
0.15	0.14	0.5	0.2	0.20	0.25	0.2	0.15	0.6	0.1	0.13	-	1.7	0.25	25
0.2	0.32	3.0	0.7	0.30	8.4	0.3	0.25	0.9	1.6	0.20	60	6.9	0.27	36
0.4	0.32	6.3	2.7	0.30	19	0.4	0.35	1.6	3.6	0.25	95	11.2	0.26	-
2.0	0.31	15	4.5	0.34	27	0.8	0.37	4.6	7.4	0.24	105	13.7	0.29	-
4.3	0.34	24	10.0	0.33	46	2.2	0.35	10	10.3	0.23	-	21.7	0.27	-
10.7	0.33	28				7.3	0.32	21	30.0	0.25	-			
19.2	0.37	-												

*Data for modulus of surface compressibility taken from force vs area curve at a molecular area corresponding to that of the wave-damping data.

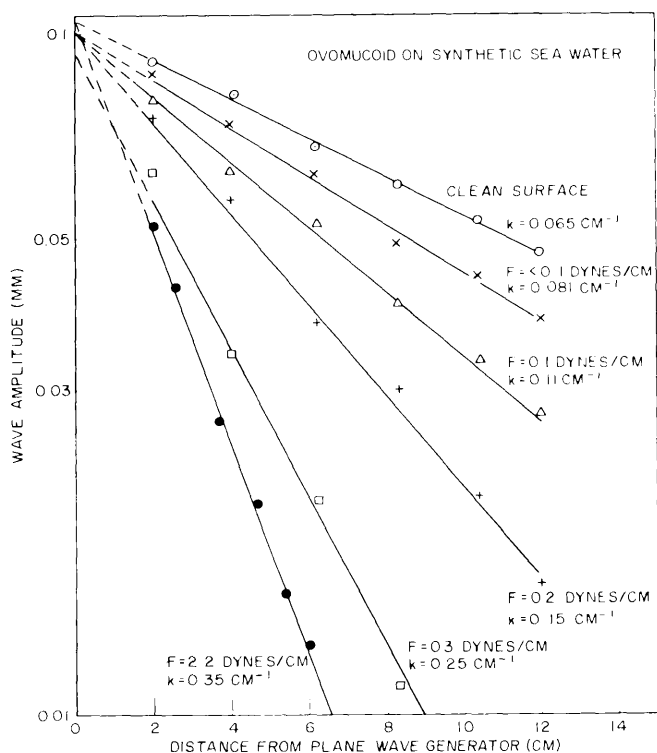


Fig. 5 - The damping of plane waves by an ovomucoid monolayer at various film pressures

The plots of damping coefficient k versus film pressure for these compounds using plane waves (Figs. 6-8) shows a relationship similar to that found for circular waves. As film pressure was initially increased, k increased gradually. Then with a further slight increase in film pressure k increased rapidly to a maximum value. This effect was quite pronounced, and the wave images faded dramatically when this stage of the experiment was reached. As shown in Figs. 6-8 and in Tables 2 and 3, this maximum remained essentially constant as the film pressure was increased further. All of the compounds examined in this fashion gave similar plots in which the maximum value of the damping coefficient was attained at film pressures of about 0.5 dyne/cm.

These data may also be represented by plotting as in Figs. 9 and 10 the damping coefficient and the film pressure against the area per adsorbed molecule in the monolayer. These figures also show an abrupt increase in the damping coefficient. For each of the compounds investigated, this change in k occurred near the region of transition of the monolayer from the gaseous diffuse state to one of greater condensation and rigidity. There is no obvious correlation between the molecular area (or molecules per unit area) and the response of the damping coefficient. In each case k changed rapidly at low values of the film pressure (Tables 2 and 3) in a region where the modulus of surface compressibility was low.

The relationship between this surface compressional modulus and the damping coefficient is represented in Fig. 11. Since the increase in k occurred at such low values of surface compression, these values were plotted on a logarithmic scale. The point at which the damping coefficient ceased to increase and then leveled off occurred so sharply that it

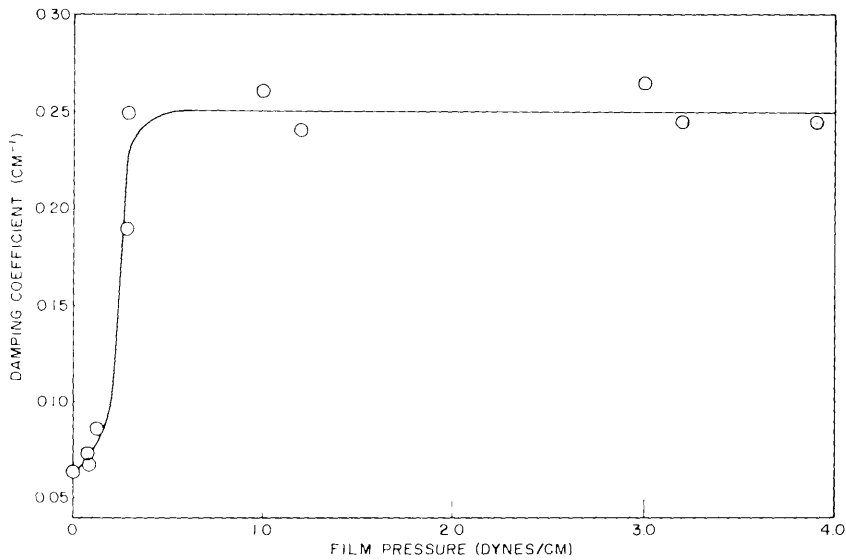


Fig. 6 - Effect of film pressure of a 9, (and 10)-phenylstearic acid monolayer on the damping coefficient for plane waves on synthetic sea water

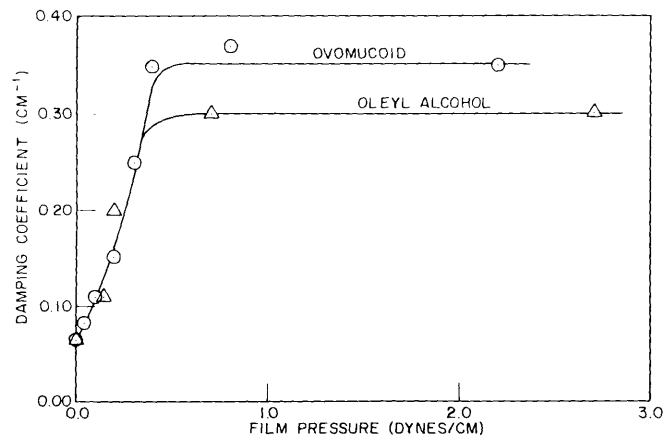


Fig. 7 - Effect of film pressure of ovomucoid and oleyl alcohol monolayers on the damping coefficient of plane waves on synthetic sea water

appeared the data points could be connected by the intersection of two straight lines. For the compounds studied these points of intersection occur at values of the compressional modulus of from 0.5 to 1.3 dynes/cm. Such variation in the compressional modulus under these circumstances may not be significant, since these values result from the measurement of very small slopes from the force vs area curves. The importance of Fig. 11 is that capillary wave damping is shown to increase rapidly at a low value of the surface compressional modulus which is essentially the same for the various monolayers studied.

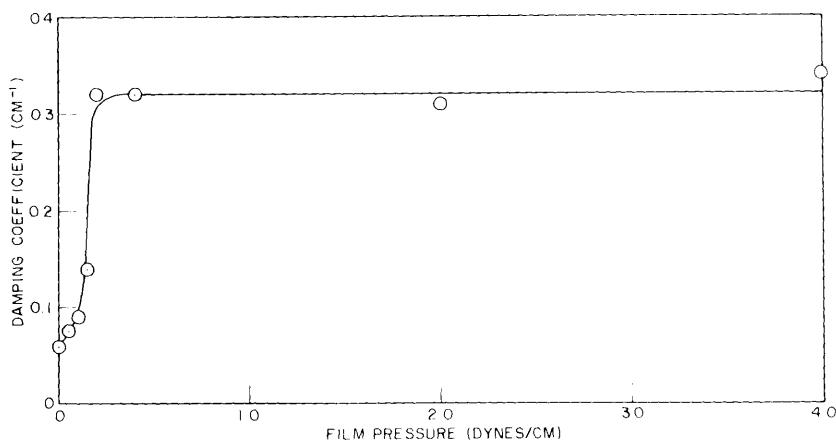


Fig. 8 - Effect of film pressure of oleic acid monolayers on the damping coefficient of plane waves on synthetic sea water

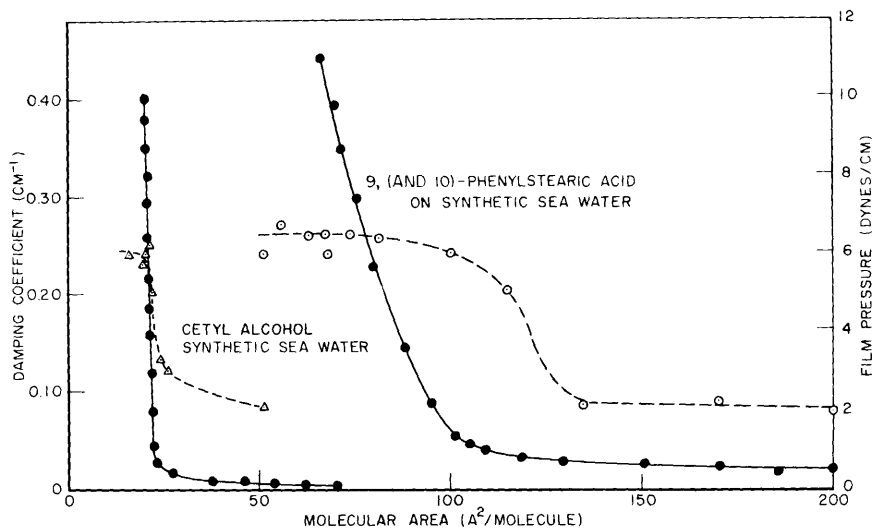


Fig. 9 - Dependence of the damping coefficient upon the area (square angstroms) per molecule of cetyl alcohol and phenylstearic monolayers (dashed lines). Corresponding film pressures vs area curves (solid lines).

DISCUSSION AND CONCLUSIONS

It has been demonstrated that the damping coefficient k for insoluble monolayers at low compression increased slowly with increasing film pressure at very low film pressures. Then between 0.1 and 0.5 dyne/cm, k increased rapidly to a maximum value. After this low film pressure was reached, further compression of the monolayer caused no significant change in the damping coefficient. A similar relationship was found between k and the modulus of surface compressibility; k increasing abruptly at low values of the compressibility modulus of from 0.2 to 0.13 dyne/cm. This effect of the film pressure and the modulus of compressibility on the damping coefficient was demonstrated by both circular and plane

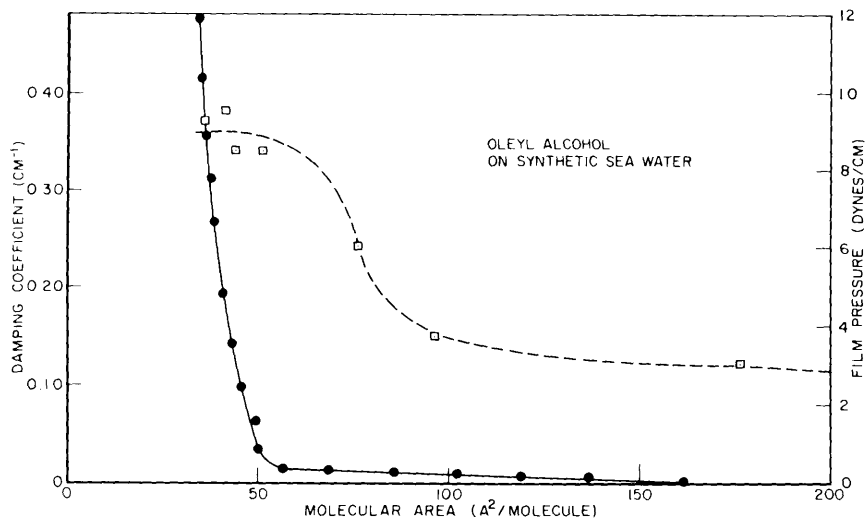


Fig. 10 - Dependence of the damping coefficient upon the area (square angstroms) per molecule of an oleyl alcohol monolayer (dashed line). Corresponding film pressure vs area curve (solid line).

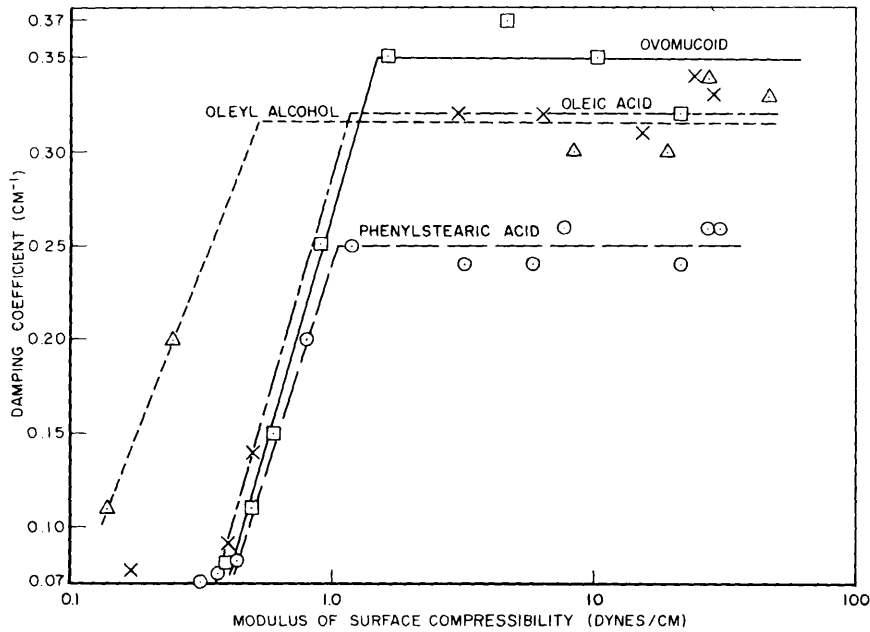


Fig. 11 - The relationship between the modulus of surface compressibility of various insoluble monolayers on synthetic sea water and the damping coefficient of plane waves

waves. However, since the plane waves possessed simpler damping characteristics, more quantitative data was obtained through the use of this wave form.

The dependence of the damping coefficient upon F and the compressibility modulus was not affected by variations in the chemical structure of the monolayer. In addition, similar results were obtained in the study of the phenylstearic acid monolayer on three different aqueous substrates which differed widely in pH and ionic concentration. Thus chemical structural effects and variations in the pH or ionic character of the substrate were not obvious.

A correlation was found between the force vs area curves and the wave-damping properties of a monolayer. By comparing the force vs area curve with a plot of damping coefficient vs area per molecule, it was found that the abrupt increase in k occurred in the neighborhood of the region of transition of the monolayer from the gaseous diffuse state to one of greater rigidity. The damping coefficient did not depend directly upon the area per molecule for it can be seen that the area per molecule of a large molecule such as ovomucoid required to cause damping would be much larger than the area per cetyl alcohol molecule necessary to give the same degree of damping.

As has been shown, however, the surface parameters of film pressure and modulus of surface compressibility appear to be of great importance in the wave damping process. The latter variable represents the differential expansion or contraction of the surface for a differential change in the film pressure at a particular area per molecule. Small changes in surface area would occur with the passage of the capillary waves in the form of local expansions and compressions. The adsorbed surface molecules would have to move laterally as these changes in area occur. In addition to the water molecule directly bonded to the adsorbed surface molecule there would be a number of water molecules associated through hydrogen bonding which would have to move correspondingly. The viscous drag associated with the oscillatory movement of this monolayer-water system would withdraw energy from the rippled water surface and result in a damping of the capillary waves.

REFERENCES

1. Davies, J.T., Chemistry and Industry (May 26):906 (1962)
2. Banting, J.D., "The Influence of Oil on Water," Report of the Third International Life-Boat Conference, Rotterdam and Amsterdam, Holland, June 21-24, 1932
3. Thomson, J., Phil. Mag. 4th Series 24:247 (1862)
4. Pockels, A., Nature 43:437 (1891)
5. Aitken, J., Proc. Royal Soc., Edinburgh 12:56-75 (1884)
6. Reynolds, Brit. Ass. Rep. (Paper i 409) 1880
7. Lamb, H., "Hydrodynamics," 6th ed., New York, Dover Press, p. 631, 1945
8. Shuleikin, V.V., "Fizika Morya," 3rd ed., Izdatel'stvo Akademii Nauk SSR, Moscow, pp. 786-819, 1953
9. Dietz, R.S., and LaFond, E.C., J. Marine Res. 9:69 (1950)
10. Lumby, J.R., and Folkard, A.R., Bull. Inst. Oceanog. No. 1080, 1-19, June 12, 1956
11. Cox, C., and Munk, W., J. Marine Res. 14:63 (1955)
12. Langmuir, I., Science 87:119 (1938)
13. Adam, N.K., Proc. Royal Society (London) B-122:134 (1937)
14. Ewing, G., J. Marine Res. 9:161 (1950)
15. Goodrich, F.C., J. Phys. Chem. 66:1858 (1962)
16. Goodrich, F.C., Proc. Royal Society A260:503 (1961)
17. Vines, R.G., Aus. J. Physics 13:43 (1960)
18. Tailby, S.R., and Portalski, S., Trans. Inst. Chem. Engs. (London) 39:328 (1961)
19. Kafesjian, R., Plank, C.A., and Gerhard, E.R., Am. Inst. Chem. Engs., Journal 7:463 (1961)
20. Davies, J.T., and Bradley, P.J., Research Project in Dept. of Chemical Engineering Cambridge, 1960
21. Van den Tempel, M., Van Voorst Vader, F., and Jonkman, R.M., J. Phys. Chem. (to be published)
22. Dorrestein, R., Proc. Acad. Sci. Amst. B54:260, 350 (1951)

23. Lord Kelvin, *Phil. Mag.* 4th Series 42:368 (1871)
24. Davies, J.T., and Rideal, E.K., "Interfacial Phenomena," New York, Academic Press, pp. 265-274, 1961
25. Schulman, J.H., and Teorell, T., *Trans. Faraday Soc.* 34:1337 (1938)
26. Schooley, A.H., "The Ripple Tank as an Aid to Phase-Front Visualization," NRL Report 3559, October 15, 1949
27. Lord Rayleigh, *Phil. Mag.* 5th Series 30:386 (1890)
28. Archer, R.J., and La Mer, V.K., *J. Phys. Chem.* 59:200 (1955)
29. "Lubricants, Liquid Fuels and Related Products; Methods of Inspection Sampling and Testing," Federal Test Method Standard, Method 4011.3, May 12, 1958
30. Dervichian, D.G., *J. Phys. Radium* 6 (7):221 (1935)
31. Harkins, W.D., and Anderson, T.F., *J. Am. Chem. Soc.* 59:2189 (1937)
32. Ruysen, R., *Bull. Soc. Chem. Belgium* 54:149 (1945)
33. Augenstine, L.G., Thesis, U. of Illinois (1956)
34. Fox, H.W., and Zisman, W.A., *Rev. Sci. Instr.* 19:274 (1948)
35. Bultman, J.D., "A Force-Area Study of Ovomuroid Films," NRL Report 5719 December 6, 1961

* * *